IEEE Photonics Journal
An IEEE Photonics Society Publication

Open Access

# Temporary Optical Coupler for Optical Cable Re-Routing Without Service Interruption

Volume 10, Number 3, June 2018

Takui Uematsu
Takanori Kiyokura
Hidenobu Hirota
Hiroyuki Iida
Tomohiro Kawano
Tetsuya Manabe

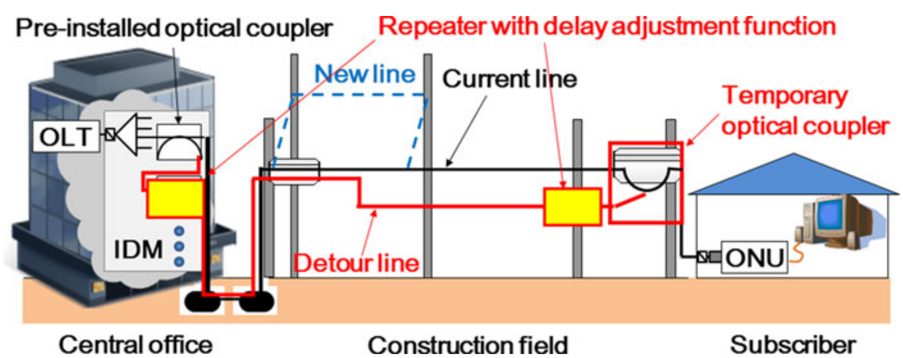


DOI: 10.1109/JPHOT.2018.2823747
1943-0655 © 2018 IEEE

# Temporary Optical Coupler for Optical Cable Re-Routing Without Service Interruption

**Takui Uematsu, Takanori Kiyokura, Hidenobu Hirota, Hiroyuki Iida, Tomohiro Kawano, and Tetsuya Manabe**

Access Network Service Systems Laboratories, NTT Corporation, Tsukuba 305-0805, Japan

*DOI:10.1109/JPHOT.2018.2823747*
*1943-0655 © 2018 IEEE. Translations and content mining are permitted for academic research only. Personal use is also permitted, but republication/redistribution requires IEEE permission. See http://www.ieee.org/publications standards/publications/rights/index.html for more information.*

Manuscript received February 27, 2018; revised March 30, 2018; accepted April 3, 2018. Date of publication April 6, 2018; date of current version April 27, 2018. Corresponding author: Takui Uematsu (e-mail: uematsu.takui@lab.ntt.co.jp).

**Abstract:** We design a temporary optical coupler to obtain high injection and extraction efficiencies while keeping the bending loss low with the aim of realizing optical cable re-routing without service interruption. The temporary optical coupler injects/extracts signal lights into/from a fiber by using fiber bending. The extraction efficiency is improved by using a double-clad fiber or a graded-index fiber for light injection and extraction while the injection efficiency is maintained compared with that of a conventional temporary optical coupler that uses a single-mode fiber. This improvement enables us to realize an optical cable re-routing operation support system that requires no service interruption.

**Index Terms:** Optical fiber applications, optical fiber couplers, optical fiber devices.

## 1. Introduction

Broadband access network services with optical fibers are extensively used throughout the world, and the number of fiber-to-the-home (FTTH) subscribers has greatly increased. Thus, it has become more important that FTTH services are always provided without interruption. On the other hand, the number of cable re-routing operations necessitated by road construction has increased along with the increase in the number of optical fiber cables in the access network. To prevent any interruption to FTTH services, we have been working on realizing optical cable re-routing operation support systems (OCROSS) that minimize the impact of optical cable re-routing operations on subscribers [1], [2].

As the first step, we proposed an OCROSS that required only a short service interruption ($<$ 30 ms) [1]. Fig. 1 shows the concept of the OCROSS in the access network. This system consists of a detour line (one of unused lines), a temporary optical coupler (TOC), and a repeater. One end of the detour line is connected to an optical coupler pre-installed in an integrated distribution module (IDM) in a central office. The other end of the detour line is connected to a repeater. The TOC can inject/extract light into/from a bent fiber, and it realizes an optical coupler temporarily at any point without the need to cut the fiber [3]–[8]. The repeater amplifies optical downstream signals (wavelengths: 1490 and 1550 nm) from the optical line terminal (OLT) through the detour line and optical upstream signals (wavelength: 1310 nm) from the optical network unit (ONU) via

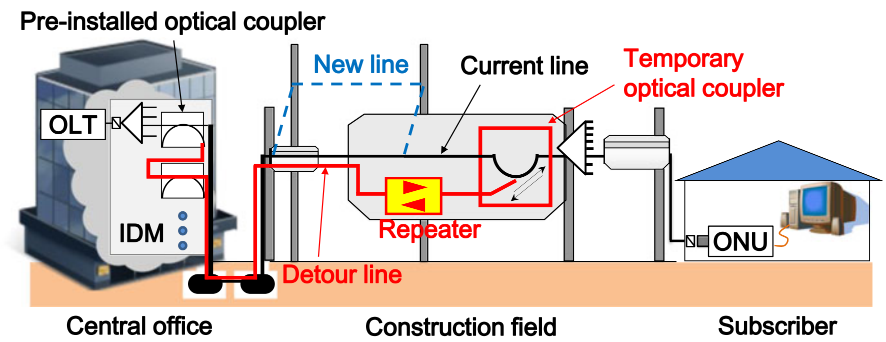


Fig. 1. Concept of OCROSS that requires only a short service interruption in a typical FTTH access network. OLT: optical line terminal. ONU: optical network unit. IDM: integrated distribution module.

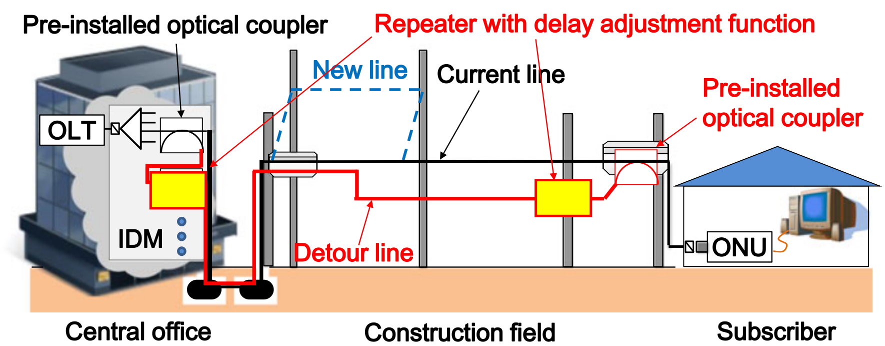


Fig. 2. Concept of OCROSS that does not require any service interruption in a typical FTTH access network.

the TOC. This system switches the route of the optical signals from the current line to the detour line by using the TOC and achieves optical cable re-routing with only a short service interruption.

Fig. 2 shows the concept behind an OCROSS that does not need any service interruption [2]. This system consists of a detour line, two optical couplers pre-installed in the IDM and near the ONU, and a pair of repeaters with a delay adjustment function. The main technologies are precise delay measurement between the current and detour lines, and the variable delay adjustment of the detour line. This system temporarily duplicates the current line with the detour line, and then it realizes optical cable re-routing without service interruption. However, this system requires the installation of an optical coupler near the ONU because the optical coupler is not installed in existing access network facilities. Service is interrupted when the optical coupler is installed.

We then develop an OCROSS that combines the above two approaches as shown in Fig. 3. This system realizes an optical coupler near the ONU by using the TOC. This approach allows us to install the optical coupler without service interruption if the TOC has a sufficiently low bending loss to maintain the transmission system. We designed the bending condition of the TOC to realize a TOC with a low bending loss [9]. However, the injection and extraction efficiencies decreased along with the decrease in the bending loss of the TOC. The decrease in the injection and extraction efficiencies means that the optical power injected into the ONU and the repeater becomes lower than the minimum sensitivity of the ONU and the repeater. Therefore, the injection and extraction efficiencies should be improved while keeping the bending loss low.

In this paper, to improve the efficiency, we design a TOC that uses a double-clad fiber (DCF) [10] or a graded-index fiber (GIF). We demonstrate that the extraction efficiency is enhanced by using a DCF or a GIF while the injection efficiency is maintained compared with that of a conventional

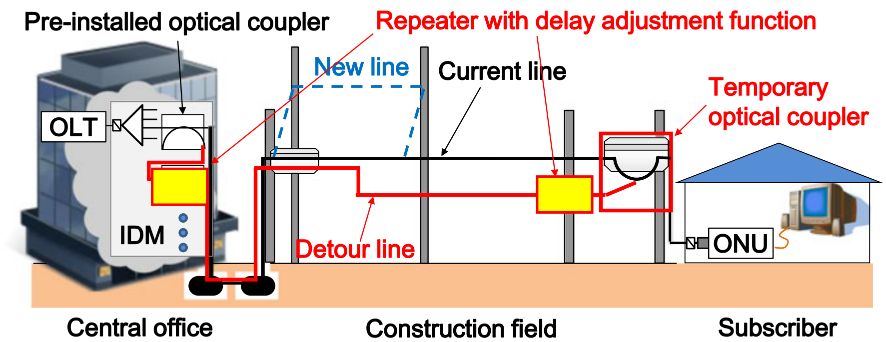


Fig. 3. Our proposed concept for an OCROSS that does not require any service interruption in a typical FTTH access network.

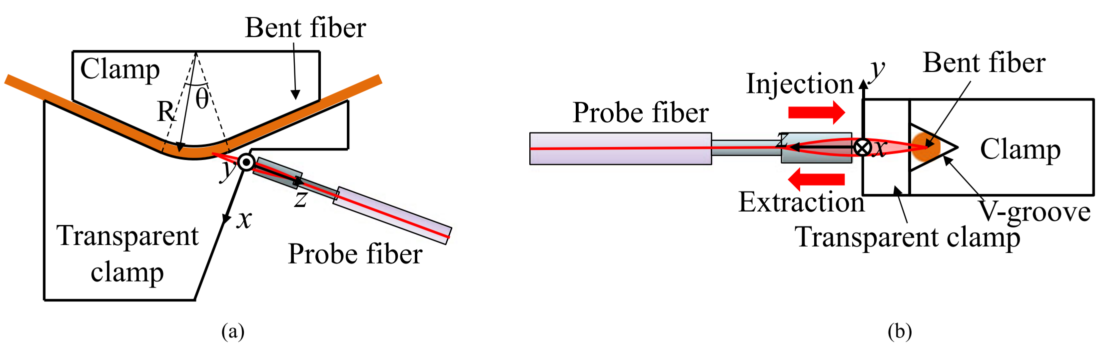


Fig. 4. Structure of temporary optical coupler: (a) top view and (b) side view.

TOC that uses a single-mode fiber (SMF). Our improvement enables us to realize our proposed OCROSS that does not require any service interruption.

## 2. Temporary Optical Coupler

Fig. 4 shows the structure of a TOC. We use convex and concave clamps to bend a fiber with the correct bending radius $R$ and angle $\theta$. We designed the bending condition to achieve high injection and extraction efficiencies and a low fiber failure probability [9]. We set the maximum bending loss at 2.0 dB at a wavelength of 1550 nm not to interrupt service. We then choose $R = 2$ mm and $\theta = 20^\circ$ [9] in this paper. The leakage power ratio of the bend region is about $-4.5$ dB, which corresponds to the estimated maximum extraction efficiency (see [9, Fig. 7]). The concave clamp is made of optically transparent plastic. The V-groove of the convex clamp is designed to keep the fiber in the correct position. The refractive index of the transparent plastic should be the same as that of the fiber coating to avoid any reflection of the leaked light at the boundary between the coating of the bent fiber and the transparent clamp. The probe fiber is used to inject/extract light into/from the bent fiber and is placed so that the highest injection and extraction efficiencies are obtained. A graded-index (GRIN) lens is spliced to the probe fiber to focus the leaked light from the bent fiber onto the core of the probe fiber and the injected light from the probe fiber onto the core of the bent fiber. The probe fiber is connected to various devices such as the repeater of our proposed OCROSS and a traffic monitoring system [9].

To realize our proposed OCROSS, the injection and extraction efficiencies should be improved while keeping the bending loss low. However, the injection and extraction efficiencies decrease along with the decrease in the bending loss of the TOC. Fig. 5 shows the Injection and extraction efficiencies of a conventional TOC compared with the requirements for realizing our proposed

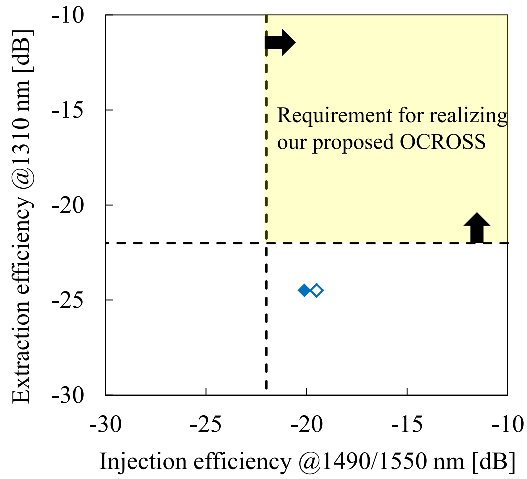


Fig. 5. Injection and extraction efficiencies compared with the requirement for realizing our OCROSS, which requires no service interruption. The wavelengths were 1310 nm for the extraction efficiency, and 1490 and 1550 nm for the injection efficiency. Closed and open symbols represent the injection efficiencies for wavelengths of 1490 and 1550 nm, respectively. Dashed lines represent the requirements for the injection and extraction efficiencies.

OCROSS. The wavelengths were 1310 nm for the extraction efficiency, and 1490 and 1550 nm for the injection efficiency. This is because the light injected into the current line by using the TOC is the downstream signal light from the OLT at wavelengths of 1490 and 1550 nm, while the extraction light from the current line is the upstream signal light from the ONU. The injection and extraction efficiencies have to exceed $-22$ dB [1], but they do not meet the requirements. The extraction efficiency should be improved by more than 2.5 dB while the decrease in the injection efficiencies is less than 2 dB to meet the requirements.

## 3. Probe Fiber Design

In the conventional TOC, an SMF is used as a probe fiber [1], [8]. Fig. 6 shows the field distributions at $y = 0$ obtained when using the beam propagation method (BPM) for extraction and injection. The leaked light from the bent fiber is focused onto the core of the SMF probe, but part of the leaked light is diffused outside the core. The extraction efficiency will be improved when a fiber with a large core is used as the probe fiber, because it captures the diffused leaked light. However, the injection efficiency decreases when a large-core fiber is used because the injected light cannot be focused onto the core of the bent fiber. In this paper, we use a DCF and a GIF, which both function as large-core and small-core fibers, to obtain both high extraction and injection efficiencies.

### *3.1 Double-Clad Fiber Probe*

Fig. 7 shows the refractive index profile of a DCF. The DCF has both a single-mode (SM) core and a multi-mode (MM) core. Figs. 8 and 9, respectively, show schematics and the effective refractive indices for light extraction from a bent fiber and light injection into it with a DCF probe. The DCF works as a large-core multi-mode fiber (MMF) corresponding to the extraction mode shown in Fig. 9 when leaked light is received from the bent fiber, while it functions as an SMF corresponding to the injection mode shown in Fig. 9 when light is injected from an SMF and into the core of the bent fiber. Fig. 10 shows field distributions for extraction and injection when the probe fiber is the DCF. The calculation condition is the same as with the SMF probe. A commercial DCF with SM core and MM core diameters of 9 and 105 $\mu$m, respectively, was used because the extraction efficiency converges to the maximum value when the core diameter is more than 62.5 $\mu$m [9]. The GRIN lens

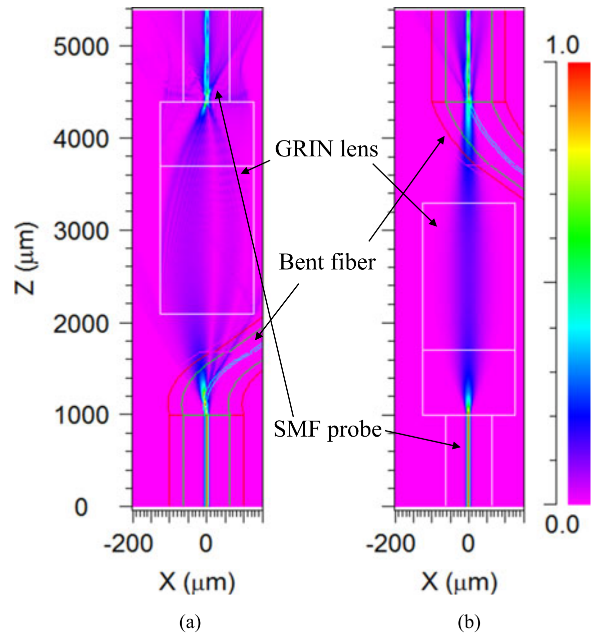


Fig. 6. Field distributions at $y = 0$ obtained using the BPM with an SMF probe for (a) extraction and (b) injection. $R = 2.0$ mm, $\theta = 20$ degrees. The diameter of the GRIN lens is 0.25 mm. The cladding and coating diameters of the bent fiber were 0.125 and 0.25 mm, respectively. The wavelength was 1550 nm. GRIN lens was designed so that the highest injection efficiency was obtained at a wavelength of 1550 nm.

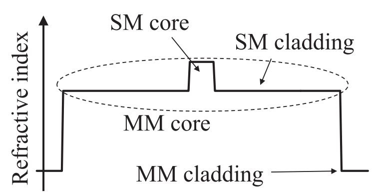


Fig. 7. Schematic of DCF index profile.

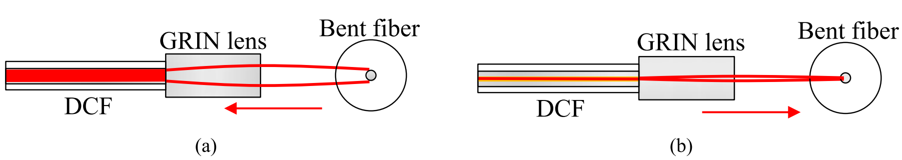


Fig. 8. Schematic of (a) extraction and (b) injection with DCF probe fiber.

was designed so that the highest injection efficiency was obtained at a wavelength of 1550 nm. We confirmed that the DCF worked as a large-core fiber for the extraction, and the extraction efficiency was improved by 7.5 dB by using the DCF probe rather than the SMF probe while the injection efficiency with the DCF was the same as that with the SMF.

### 3.2 Graded-Index Fiber Probe

Fig. 11 shows the refractive index profile of a GIF. The index profile decreases as the GIF radius increases. Fig. 12 shows the effective refractive indices for the injection and extraction processes for

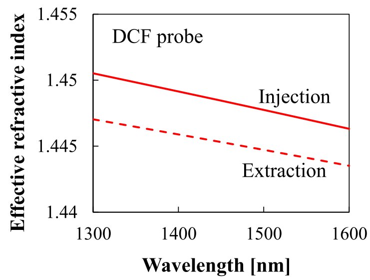


Fig. 9. Effective refractive indices for injection and extraction processes for DCF probe. Solid and dashed lines represent the effective refractive indices for injection and extraction, respectively.

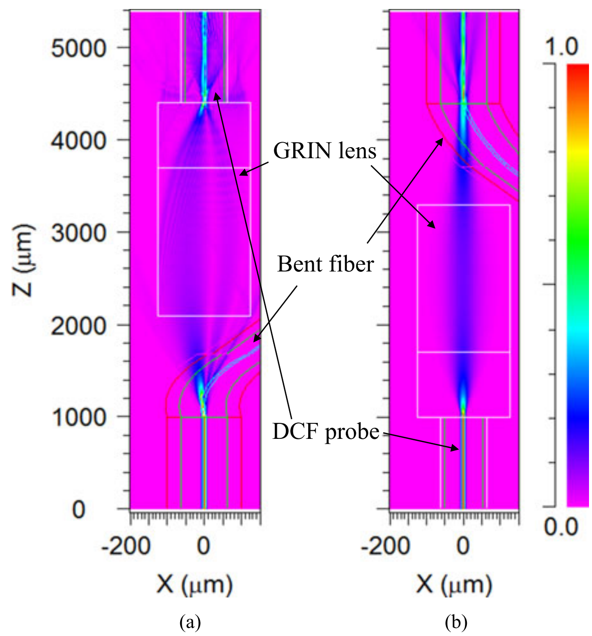


Fig. 10. Field distributions at $y = 0$ obtained with the BPM and a DCF probe for (a) extraction and (b) injection. The calculation condition is the same as in Fig. 6.

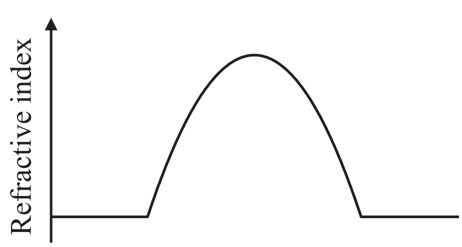


Fig. 11. Schematic of GIF index profile.

a GIF probe. In the injection process, light injected from an SMF combines with GIF modes that are largely similar to the SMF fundamental mode corresponding to the injection mode shown in Fig. 12. On the other hand, in the extraction process, the leaked light from the bent fiber combines with the extraction mode, which has many GIF modes. Therefore, the GIF probe works as both a large-core and a small-core fiber in the same way as the DCF probe. Fig. 13 shows field distributions for

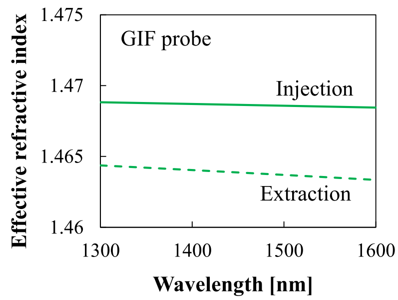


Fig. 12. Effective refractive indices for injection and extraction processes for GIF probe. Solid and dashed lines represent the effective refractive indices for injection and extraction, respectively.

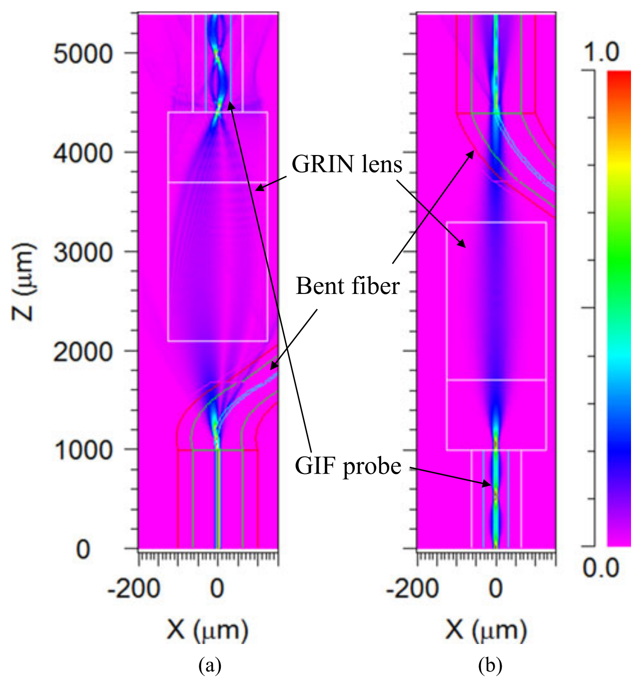


Fig. 13. Field distributions at $y = 0$ obtained with the BPM using a GIF probe for (a) extraction and (b) injection. The calculation condition is the same as in Fig. 6.

extraction and injection when the probe fiber is the GIF. A commercial GIF with a radius of 62.5 $\mu$m was used in the simulation. Fig. 13 shows that the GIF worked as a large-core MMF for extraction while it worked as a small-core fiber for injection in the same way as the DCF probe. From the simulation results, we confirmed that the extraction efficiency was improved by 7.8 dB by using the GIF probe rather than the SMF probe while the injection efficiency with the GIF was the same as that with the SMF.

### *3.3 Comparison of Fiber Probe*

In this section, we compare the SMF, DCF, and GIF probes by using the simulated BPM results. Fig. 14 shows the improvement in the extraction and injection efficiencies with the DCF and GIF probes compared with results obtained with the SMF probe. The extraction efficiencies were improved by 7.2 to 9.4 dB over a 1300 to 1600 nm wavelength range. On the other hand, the injection efficiency with the DCF probe was the same as that with the SMF probe. The injection efficiency

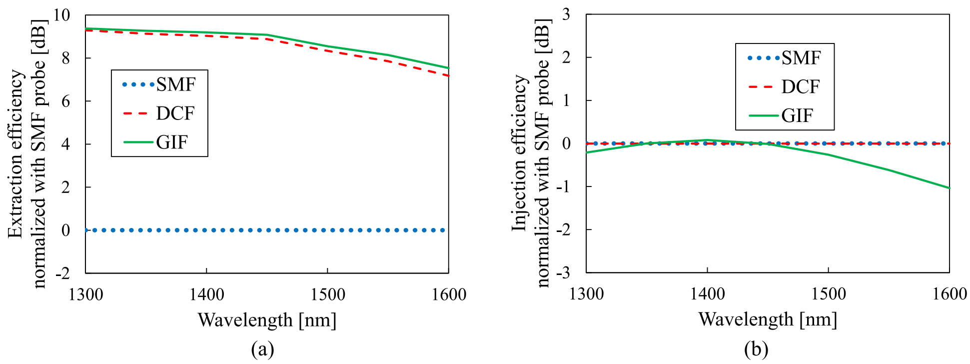


Fig. 14. Simulated improvement of (a) extraction and (b) injection efficiencies compared with the result obtained using an SMF probe. Dashed lines represent the requirements for realizing our proposed OCROSS.

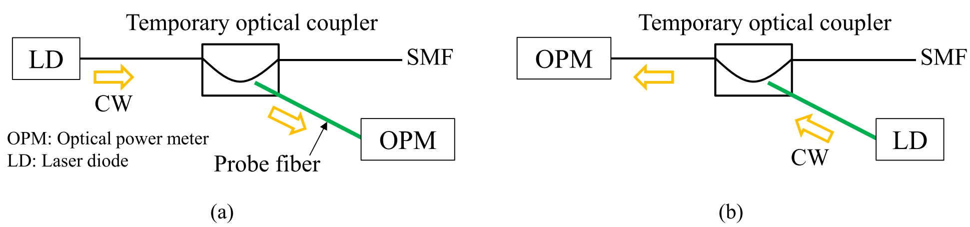


Fig. 15. Experimental setup for measuring (a) extraction and (b) injection efficiencies. The probe fiber is the SMF, DCF, or GIF designed in Section 3.

for the GIF probe was slightly dependent on wavelength, and it was degraded by about 1 dB at a wavelength of 1600 nm. This was because the mode field diameter of the injection light in the GIF was dependent on wavelength. The above results show that the DCF and GIF probes improve extraction efficiency by over 7 dB while maintaining injection efficiency, and the requirements of the extraction and injection efficiencies are met.

## 4. Experimental Results

We measured the extraction and injection efficiencies with the experimental setup shown in Fig. 15. The probe fiber was the SMF, DCF, or GIF designed in Section 3. The sample fiber was compatible with ITU−T G.652 [11]; the coating diameter was 250 $\mu$m. The bending losses of the TOC were 0.38, 1.0, and 2.0 dB at wavelengths of 1310, 1490, and 1550 nm, respectively.

Fig. 16 shows the experimentally obtained extraction and injection efficiencies normalized with the SMF probe at wavelengths of 1310, 1490, and 1550 nm. Dashed lines represent the simulated results shown in Fig. 14. The measured injection efficiencies for the DCF and GIF probes were about the same as that for the SMF probe. The measured extraction efficiency for the DCF probe was enhanced by 6.0 to 7.1 dB compared with the extraction efficiency of the SMF probe as we expected from the simulation. The measured extraction efficiency for the GIF probe was also enhanced by 7.6 to 9.5 dB compared with that of the SMF probe. The measured result for the GIF probe generally matches the simulated result, while there is some difference between the simulated and measured results for the DCF probe. The difference between the measured and simulated results is mainly due to the transmission loss of the DCF probe, which is estimated 1 to 2 dB. The difference is also due to GRIN lens manufacturing errors, which are estimated to be 0.5 to 1 dB.

We also measured the bit error rate (BER) to evaluate the quality of the signals passing through the TOC. Fig. 17(a) shows the experimental setup for the BER measurement for extraction. We

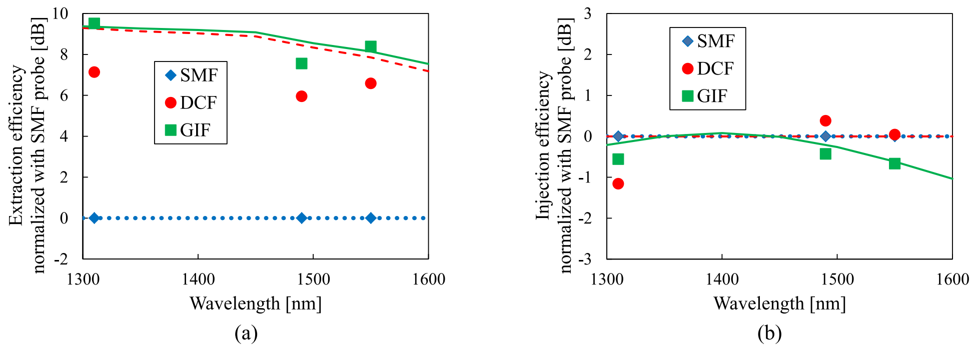


Fig. 16. Measured improvement in (a) extraction and (b) injection efficiencies compared with those obtained with the SMF probe at wavelengths of 1310, 1490, and 1550 nm. Dashed lines represent the simulated results shown in Fig. 14.

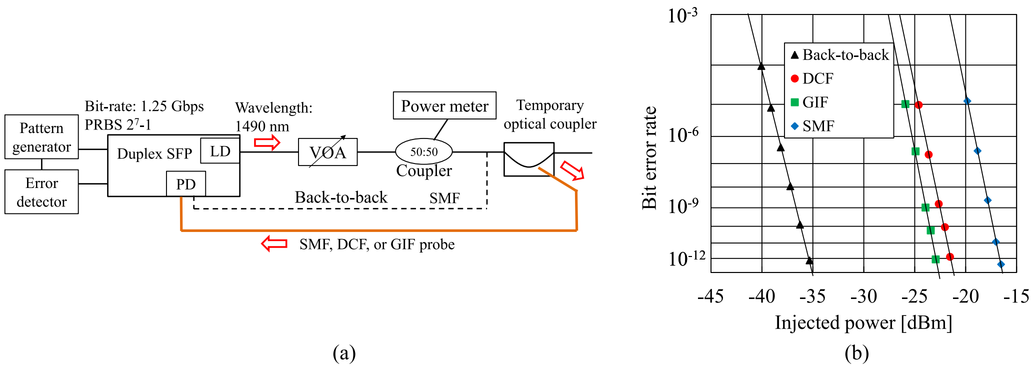


Fig. 17. BER measurement for extraction: (a) experimental setup and (b) BER at a wavelength of 1490 nm. The probe fibers are directly connected to a commercial duplex SFP transceiver that complies with Gigabit Ethernet as specified in IEEE Std. 802.3. The injected power in (b) corresponds to the power monitored with a power meter as shown in (a).

set the bit rate at 1.25 Gbps because our proposed OCROSS were employed for Gigabit Ethernet passive optical network. We used a commercially available duplex small form factor pluggable (SFP) transceiver, which complied with Gigabit Ethernet as specified in IEEE Std. 802.3. The probe fibers were 2 m long to suppress modal dispersion and were directly connected to the SFP receiver. In the receiver of the duplex SFP transceiver, light received by and transmitted through the probe fiber was focused by a ball lens onto an avalanche photodiode with an active area of about 55 $\mu$m. The BER of a back-to-back transmission was also measured via an SMF without a TOC. Fig. 17(b) shows the experimental BER result at a wavelength of 1490 nm. The power penalties at a BER of $10^{-12}$ compared with the back-to-back transmission were 18.7, 13.9, and 12.5 dB for SMF, DCF, and GIF probes, respectively. These power penalties were predominantly due to the extraction efficiencies of $-18.7$, $-12.9$, and $-11.3$ dB for the SMF, DCF, and GIF probes, respectively. The coupling loss between the probe fiber and the photodiode of the SFP receiver was also included in the power penalty of the DCF and GIF probes. The power penalty was improved by about 4.8 and 6.2 dB by using the DCF and GIF probes, respectively, although there was a coupling loss of about 1.0 or 1.2 dB for the DCF and GIF probes, respectively. The coupling loss will be reduced by focusing the light from the probe onto the photodiode with the designed lenses. Similarly, Fig. 18 shows the BER measurement for injection. The power penalties for the SMF, DCF, and GIF probes were 18.3, 19.1, and 19.9 dB, respectively. The main reasons for the differences between these power penalties are GRIN lens manufacturing errors.

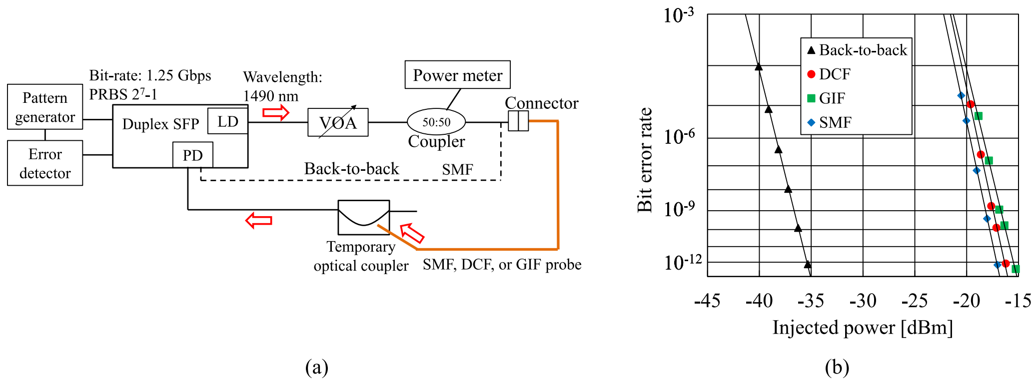


Fig. 18. BER measurement for injection: (a) experimental setup and (b) BER at a wavelength of 1490 nm.

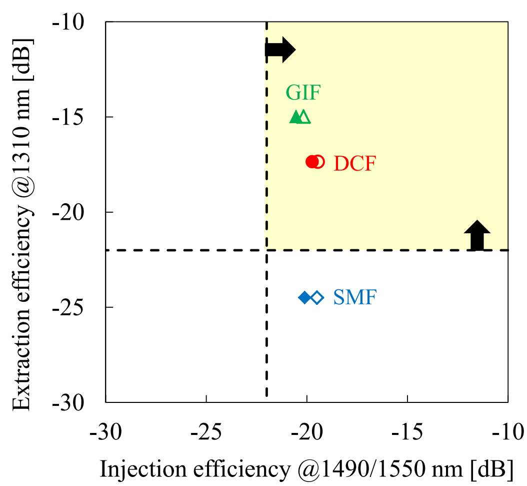


Fig. 19. Injection and extraction efficiencies compared with the requirement for realizing our OCROSS, which requires no service interruption. Closed and open symbols represent the injection efficiencies for wavelengths of 1490 and 1550 nm, respectively.

Finally, we discuss the feasibility of our proposed OCROSS, which requires no service interruption. Fig. 19 shows the Injection and extraction efficiencies compared with the requirements for realizing our proposed OCROSS. The injection and extraction efficiencies meet the requirements by using the DCF and GIF probes. Therefore, the proposed OCROSS can be realized by using the designed TOC.

## 5. Conclusions

We designed the probe fiber of a TOC to obtain high injection and extraction efficiencies while keeping the bending loss low with a view to realizing our proposed OCROSS, which requires no service interruption. We demonstrated that by using DCF and GIF probes, respectively, the extraction efficiencies increased by over 6.0 and 7.6 dB compared with that obtained with a conventional SMF probe, while the injection efficiencies were decreased by less than 1.2 and 0.7 dB. We also measured the BER, and confirmed that the power penalty induced by the TOC was about 1.0 dB. Finally, we discussed the feasibility of our proposed OCROSS when using the TOC. The designed TOC enabled us to meet the requirement for realizing optical cable re-rerouting without service interruption.

## References

[1] T. Manabe, T. Kawano, T. Kiyokura, T. Uematsu, and H. Hirota, "Optical cable re-routing operation support system with a short service interruption," in *Proc. 2017 UL Int. Cable Connectivity Symp. China*, Apr. 2017, presented at 10-1. [Online]. Available: http://www.ulandiwcschina.org/iwcschina2017-1.4007121/t002-1.4007194/f012-1.4007217/a066-1.4007230/ap125-1.4007231

[2] T. Manabe, K. Noto, M. Inoue, H. Watanabe, and Y. Koshikiya, "Optical cable re-routing operation support system without service interruption," in *Proc. 66th Int. Cable Connectivity Symp.*, Oct. 2017, pp. 733–738.

[3] M. D. Feuer and V. A. Vaishampayan, "Clip-on fiber identifier using digital lightpath labels," *Proc. SPIE*, vol. 7632, 2009, Art. no. 763220.

[4] T. Matsui, K. Nakajima, K. Toge, T. Kurashima, and M. Tsubokawa, "Fiber identification technique based on mechanically-induced long-period grating for bending-loss insensitive fibers," *J. Lightw. Technol.*, vol. 28, no. 24, pp. 3556–3561, Dec. 2010.

[5] K. Matsuoka, S. Niimi, M. Miyamoto, and H. Sugawara, "New optical fiber identifier," in *Proc. 64th Int. Cable Connectivity Symp.*, Oct. 2015, pp. 704–708.

[6] M. Shimizu, S. Takashima, and H. Kobayashi, "Identification system for optical fiber transmission operation lines with local-light injection and detection coupling system," *J. Lightw. Technol.*, vol. 10, no. 5, pp. 686–692, May 1992.

[7] Go4Fiber, "Passive fiber clip-on coupler." 2017. [Online]. Available: https://www.go4fiber.com/spec/PFC%201000.pdf

[8] H. Hirota *et al.*, "Optical cable changeover tool with light injection and detection technology," *J. Lightw. Technol.*, vol. 34, no. 14, pp. 3379–3388, Jul. 2016.

[9] T. Uematsu, H. Hirota, T. Kawano, T. Kiyokura, and T. Tetsuya, "Design of temporary optical coupler using fiber bending for traffic monitoring," *IEEE Photon. J.*, vol. 9, no. 6, Dec. 2017, Art. no. 7106013.

[10] T. Uematsu, T. Kiyokura, H. Hirota, T. Kawano, and T. Tetsuya, "High-efficiency light injection and extraction using fiber bending," in *Proc. 2017 Opt. Fiber Commun. Conf.*, Mar. 2017, Paper W2A.15.

[11] Characteristics of a Single-Mode Optical Fibre and Cable, ITU-T Rec. G. 652, Nov. 2009.